



# Ultraviolet photodissociation spectroscopy of cold, isolated adenine complexes with a potassium cation



Ji Young Baek<sup>a</sup>, Chang Min Choi<sup>a</sup>, Han Jun Eun<sup>a</sup>, Kwang Sik Park<sup>a</sup>, Myoung Choul Choi<sup>b</sup>, Jiyoung Heo<sup>c,\*</sup>, Nam Joon Kim<sup>a,\*</sup>

<sup>a</sup> Department of Chemistry, Chungbuk National University, Chungbuk 362-763, Republic of Korea

<sup>b</sup> Mass Spectrometry & Advanced Instrument Group, Korea Basic Science Institute, Ochang Center, Chungbuk 28119, Republic of Korea

<sup>c</sup> Department of Biomedical Technology, Sangmyung University, Chungnam 330-720, Republic of Korea

## ARTICLE INFO

### Article history:

Received 7 March 2015

In final form 17 June 2015

Available online 29 June 2015

## ABSTRACT

We obtain the ultraviolet photodissociation spectrum of adenine complexes with  $K^+$  ion stored in a cold ion trap. The spectrum near the origin band of the  $S_0-S_1$  transition exhibits well-resolved vibronic bands, all of which are assigned from a single isomer by UV–UV hole-burning (HB) spectroscopy. Comparing the spectrum with theoretical spectra, we determine the structure of the isomer, where  $K^+$  is bound not to 9H-adenine (A9) but to 7H-adenine (A7). We suggest that  $K^+A7$  ions are formed in solution through tautomerization, for which the energy barrier varies greatly depending on the binding site of the  $K^+$  ion on A9.

© 2015 Elsevier B.V. All rights reserved.

## 1. Introduction

Alkali metal cations play critical roles in the stability and function of DNA [1–3]. In particular, metal cations bound to nucleobases alter the electron distributions of the bases and hence their acid–base properties. These alterations may influence the hydrogen bonding and stacking interactions between nucleobases that determine the stability of DNA conformations [4,5].

To understand these effects of alkali metal cations on DNA, metal ion–nucleobase complexes have been extensively studied as a simplified model system in recent decades [6–12]. The binding energies and metalation sites of  $M^+$  ( $M = Li, Na, \text{ and } K$ ) to nucleobases were theoretically predicted [4,13,14]. The alkali metal ion affinities of nucleobases were determined from dissociation of the metal ion-bound heterodimers using mass spectrometry [15–18]. The structures of alkali metal cation–nucleobase complexes and their hydrated clusters were investigated using a combination of infrared multiphoton dissociation (IRMPD) spectroscopy and quantum theoretical calculations [19–21]. For the structures of alkali metal ion–adenine complexes ( $M^+A$ ), Rodgers and Armentrout [16] insisted that the metal cations bind most strongly to N7 of A9 ( $M^+A9$ ). However, Fridgen et al. [19] concluded that  $M^+A$

ions produced by electrospray ionization (ESI) are not  $M^+A9$  but  $M^+A7$ , where the metal ion is attached to the A7 tautomer. They attributed this discrepancy to the difference in the methods for producing  $M^+A$  ions. If the metal ion is added to A9 in the gas phase, it simply binds to A9, producing  $M^+A9$ . However, if  $M^+A$  is formed in solution, there is plenty of time for tautomerization to form the lowest energy complex,  $M^+A7$ .

Adenine is known to exist as the A9 or A7 tautomer in water with the equilibrium constant  $K = [A7]/[A9] = 0.28$  at 20 °C [22]. However, this tautomer equilibrium can be strongly influenced by the presence of metal cations. It is well established that metal cations stabilize non-canonical rare tautomers of nucleobases, which may cause the mispairing of DNA during the replication process [5]. Fortunately, the tautomerism between A9 and A7 does not occur in DNA because N9 of adenine is bound to the deoxyribose moiety. However, free adenine and guanine molecules, which are liable to undergo tautomerization, are formed by the hydrolytic degradation of nucleic acids and nucleotides and can be reconverted to purine nucleotides by a salvage pathway [23].

The tautomerism of A9 has been extensively studied as a model system for tautomerism [22,24–26]. However, the roles of the metal cations in the tautomerization, especially in the presence of water molecules, have not yet been fully understood. It has been reported that the presence of  $Na^+$  decreases both the rate and the equilibration constants of tautomerization of hydrated methylcytosine [7]. In contrast, the tautomerization process of amino–imino adenine isomer is greatly improved by the presence

\* Corresponding authors.

E-mail addresses: [jiyoungheo@smu.ac.kr](mailto:jiyoungheo@smu.ac.kr) (J. Heo), [namjkim@chungbuk.ac.kr](mailto:namjkim@chungbuk.ac.kr) (N.J. Kim).

of alkali metal cations and water [27]. It was also asserted that metal ions bound to different sites of uracil play opposite roles in the tautomerization process [11].

Here, we investigate adenine complexes with a potassium cation ( $K^+A$ ) stored in a quadrupole ion trap (QIT) at 10 K using UV photodissociation (UVPD) and UV–UV HB spectroscopy. These spectroscopic methods have provided powerful tools to elucidate the geometric and electronic structures of ions produced by ESI [28–31]. It has been determined that  $K^+A$  ions exist as a single isomer, where  $K^+$  ion binds not to A9 but to A7 in a bidentate way. To reveal the roles of  $K^+$  ion in this exclusive formation of  $K^+A7$  ions in a solution of A9 and KCl, we estimate the energy barriers for the tautomerization of  $K^+A9$  isomers solvated with water or methanol molecules using density functional theory (DFT).

## 2. Experimental details

The experimental set-up is described in detail elsewhere [32], and only a brief description is given below. A9 and KCl were purchased from Sigma–Aldrich and used without further purification. The powder samples were dissolved in methanol at a concentration of 1 mM. The mixed solution was electrosprayed into ion droplets through a nozzle floated at +3 kV. The solvent molecules in ion droplets evaporated in the heated capillary at 80 °C. The resulting ions passed through a skimmer and an octupole ion guide and were trapped for 48 ms in the QIT at ~10 K. The ions in the QIT were irradiated by a UV laser pulse and extracted to the reflectron time-of-flight mass spectrometer.

For UV–UV HB spectroscopy [31], the frequency-doubled outputs of two dye lasers pumped by Nd:YAG lasers were used as pump and probe pulses. The pump pulse was fixed at the wavenumber of a vibronic band in the UVPD spectrum, and the probe pulse scanned the wavenumber region of 35 950–36 700  $\text{cm}^{-1}$ . The time delay between the pump and probe pulses was adjusted to 4  $\mu\text{s}$ .

## 3. Computational details

The geometries of all possible configurations for  $K^+A9$  and  $K^+A7$  in the gas phase were optimized using the M06-2X functional with 6-311++G(d,p) [33]. The geometries and corresponding energies in water or methanol were computed at the same level using the dielectric continuum solvation model. The polarizable continuum model using the integral equation formalism variant (IEFPCM) [34] was employed with radii and non-electrostatic terms from the SMD solvation model [35]. The initial structure of the transition state (TS) in the tautomerization was obtained by scanning the N9–H distance of A9 and then fully optimized on the same level. The TS was confirmed by intrinsic reaction coordinate (IRC) calculation. The vibrational frequencies were computed to ensure that the geometries were in either a stationary state or TS. All calculations were performed using the GAUSSIAN 09 software [36].

## 4. Results and discussion

Figure 1a is the UVPD spectrum of  $K^+A$  ions in the cold QIT near the origin band of  $S_0$ – $S_1$  transition. This spectrum is obtained by monitoring the signal of photofragment  $K^+$  ions as a function of UV wavelength. The spectrum exhibits well-resolved vibronic bands with a full width at half maximum of ~6  $\text{cm}^{-1}$ . This result is in stark contrast to the UVPD spectrum of protonated adenine ( $H^+A$ ) [37], which shows only a broad absorption band. This broad band was attributed to its short excited-state lifetime. Thus, the well-resolved vibronic bands in Figure 1a may imply a longer excited-state lifetime of  $K^+A$  than of  $H^+A$ .

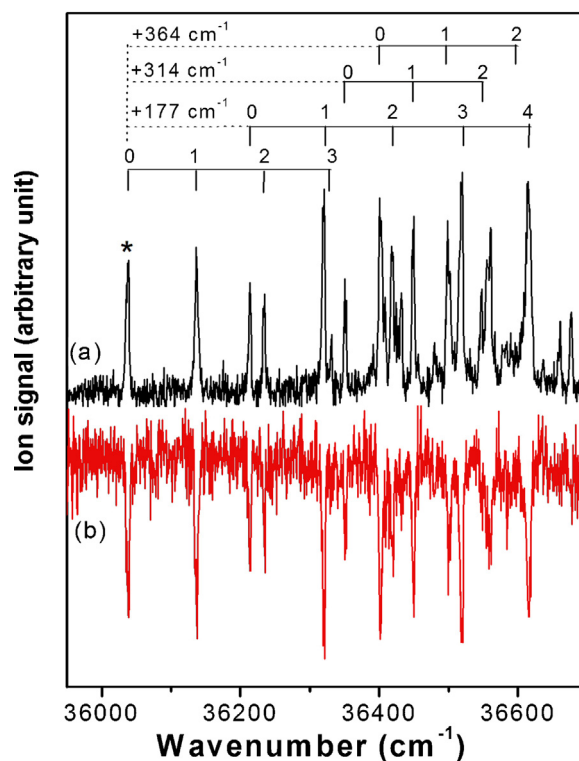


**Figure 1.** (a) UVPD and (b) UV–UV HB spectra of  $K^+A$  ions. The UV–UV HB spectrum is obtained with the pump fixed at the lowest-energy band (\*).

To determine the number of different isomers contributing to the UVPD spectrum, we obtain the UV–UV HB spectrum with the pump fixed at the lowest-energy band (Figure 1b). All vibronic bands in the UVPD spectrum are observed in the UV–UV HB spectrum, which indicates the contribution of only a single isomer to the spectrum. For information on the structure of the isomer, we calculate the relative energies of the  $K^+A$  isomers using DFT.

Figure 2 shows the low-energy structures of  $K^+A$  isomers in the gas phase.  $K^+A7a$  ion is predicted as the lowest-energy isomer (Table 1). Even in water and methanol,  $K^+A7a$  is more stable than  $K^+A9$  isomers by 8–11 kJ/mol and 16–21 kJ/mol, respectively. These results imply that the single isomer might be  $K^+A7a$  formed in solution through tautomerization.

To further confirm that  $K^+A7a$  gives rise to the UVPD spectrum, we simulate the electronic spectra of  $K^+A7a$ ,  $K^+A7b$ ,  $K^+A9b$ , and  $K^+A9c$  using time-dependent density functional theory (TDDFT) at the M06-2X/6-311++G(d,p) level (Figure 3 and Figure 1S in Supplementary data). The electronic spectrum of  $K^+A9a$  cannot be simulated due to its dissociative nature in the  $S_1$  state. We also

**Table 1**  
Relative energies and Gibbs free energies of  $K^+A$  isomers<sup>a</sup>.

	$\Delta E^b$	$\Delta G_g^c$	$\Delta G_w^d$	$\Delta G_m^e$
$K^+A7a$	0	0	0	0
$K^+A7b$	80.6	80.1	16.3	30.7
$K^+A9a$	44.2	43.2	7.8	16.4
$K^+A9b$	35.1	35.9	11.0	20.6
$K^+A9c$	35.3	36.8	10.1	19.3
$K^+A3a$	59.6	58.3	24.8	31.3
$K^+A3b$	101.6	102.3	37.1	50.8
$K^+A3c$	64.3	65.0	28.8	39.4

<sup>a</sup> Unit in kJ/mol.

<sup>b</sup> Relative energies in the gas phase with the zero-point energy correction.

<sup>c</sup> Relative Gibbs free energies at 298.15 K in the gas phase.

<sup>d</sup> Relative Gibbs free energies at 298.15 K in water.

<sup>e</sup> Relative Gibbs free energies at 298.15 K in methanol.

Download English Version:

<https://daneshyari.com/en/article/5379680>

Download Persian Version:

<https://daneshyari.com/article/5379680>

[Daneshyari.com](https://daneshyari.com)